Phase Equilibria and Transition Mechanisms in High-Pressure AgCl by Ab Initio Methods

Michele Catti* and Luca Di Piazza

Dipartimento di Scienza dei Materiali, Università di Milano Bicocca, via Cozzi 53, 20125 Milano, Italy

Received: October 27, 2005

The theoretical study of pressure-driven phase transformations by means of ab initio quantum mechanical methods, in the frame of the extended Landau approach, is considered. A specific application to AgCl is presented: the system shows, on increasing pressure, four polymorphs with rock salt- ($Fm\bar{3}m$), KOH- ($P2_1/m$), TlI- ($Cmcm$), and CsCl- ($Pm\bar{3}m$) type structures. The method of constant-pressure enthalpy minimization was used for all phases, by fully relaxing the corresponding crystal structures. Periodic ab initio energy calculations were performed by the CRYSTAL03 code, employing a DFT-GGA-PBE functional with a localized basis set of Gaussian-type functions. The three phase transitions were predicted to occur at 3.5, 6.0, and 17.7 GPa, respectively, against pressures of 6.6, 10.8, and 17 GPa from literature experimental results. The rock salt- to KOH-type and KOH- to TlI-type displacive transformations show a weak first-order character. The TlI- to CsCl-type reconstructive transition is sharply first-order, and its kinetic mechanism was studied in detail on the basis of a $P2_1/m$ pathway, similar to that previously found for the rock salt- to CsCl-type transformation of NaCl. An activation enthalpy of 0.011 eV was found at the equilibrium pressure of 17.7 GPa.

Introduction

Solid-to-solid phase transformations, whether driven by temperature or by pressure or by chemical composition, show a very extensive phenomenology which still challenges scientists to a deep theoretical comprehension. In this respect, the atomic-scale pathway from a crystal structure to another has been mostly modeled as a collective motion of atoms preserving some kind of long-range translational symmetry, though a subset of the space-group symmetry operators of each phase may be lost. This fundamental assumption is the base of Landau's theory and of all attempts to rationalize structural phase transitions on the basis of group theoretical considerations.[1,2] The foundation of this approach is the atomistic "continuity" of the transformation, expressed by the concept of order parameter ξ, which measures the dissymmetry of the low-symmetry structure quantitatively (e.g., cf. the case of displacive transitions[3]).

These ideas have been extended in the last years also to apparently discontinuous processes, such as reconstructive phase transitions, where no group/subgroup relations are observed between the symmetries of the two phases involved.[4] In this case, an intermediate structural state is postulated, whose symmetry is a common subgroup of the space groups of both phases. Thus, the continuous character of the atomistic process is recovered at the level of the intermediate state, where an order parameter can be defined, ranging between two end values which correspond to the two high-symmetry polymorphs. Intermediate values of the order parameter correspond to unstable, or possibly metastable, states unlike the stable thermodynamic states ("phases") observed where the free energy is an absolute minimum. Such nonequilibrium states can also be simulated in the case of displacive transitions. A quantitative modeling of first-order reconstructive or displacive phase transitions can give access, in principle, to activation barriers and then to the transformation kinetics.

One should be aware, however, that not all aspects of the phase transition phenomenology can be accounted for by the extended Landau approach. In particular, the role of defects and/or diffusion processes is not considered explicitly, whereas in some cases these may just control the rate-determining step and then the kinetics of the transformation. Yet, the model of cooperative, diffusionless atomic motion can provide a partial but relevant insight also where grain boundary effects are important, because it is at least adequate to represent the atomistic mechanism inside the defect-free crystal grain.

A wide new field of applications of the long-range order model to phase transformations has been opened in recent years by the impressive progress of quantum mechanical computational tools for periodic systems. This allows one, in principle, to exploit all features of the approach in a full quantitative way, by calculating directly the thermodynamic potentials as functions of the order parameter on the basis of physical first principles. It is much simpler to do that if the relevant variable is pressure, p, rather than temperature T; for this reason, in the following, only phase transitions driven by pressure will be considered. In this case, the suitable thermodynamic potential is enthalpy $H = E + pV$, where E is the quantum mechanical ground-state crystal energy at the "athermal limit" ($T = 0$ K), and V is volume. By constant-pressure minimization of the enthalpy with respect to all structural variables for each phase involved, the corresponding $H(p)$ curves are obtained, and then, the theoretical phase diagram can be predicted. If the order parameter ξ is kept fixed and excluded from the minimization, then the $H(\xi, p)$ curves are calculated, giving access to nonequilibrium states and, possibly, to kinetics. Further, by comparing the calculated enthalpy barriers for different types of intermediate states, it is possible to detect the least-enthalpy transformation mechanism. There are several examples in the literature of studies of this kind on systems such as GaAs, SiC, ZnS, NaCl, and so forth.[5−9]

Here, an application to the case of AgCl is presented, whose high-pressure polymorphism was investigated experimentally

* Corresponding author. E-mail: catti@mater.unimib.it.

10.1021/jp056174q CCC: $33.50
Published on Web 01/07/2006

by diamond-anvil-cell synchrotron X-ray diffraction.[10,11] After surveying the previous knowledge on this system, both the thermodynamic and kinetic aspects of its phase transformations will be explored by the ab initio approach, within the theoretical frame outlined above.

The AgCl Phase Transitions

According to the Phillips scale of ionicity,[12] silver halides are ranked in the order AgCl (0.856), AgBr (0.850), and AgI (0.770), so that AgCl and AgBr overcome the critical value of 0.785 and show a sixfold coordination structure (rock salt-type) as the stable room-pressure phase, against the fourfold coordination zinc blende-type phase of silver iodide. The high-pressure transformations of AgCl were the object of a number of investigations in the past, but only the two most recent ones[10,11] could clarify completely the structures of the corresponding polymorphs. Thus, on increasing pressure, the rock salt phase ($Fm\bar{3}m$) is replaced by a monoclinic $P2_1/m$ polymorph with KOH-type structure; then an orthorhombic (*Cmcm*) TlI-type phase with CN = 7, and eventually, the eightfold coordination CsCl-type ($Pm\bar{3}m$) polymorph follow. The three corresponding phase transitions were reported to occur at 8, 13, and 17 GPa in ref 10, whereas the authors of ref 11 gave values of 6.6 and 10.8 GPa for the rock salt/KOH and KOH/TlI transformations, respectively, but did not reach the pressure where the third transition occurs. The first two transitions have a displacive character ($P2_1/m$ is subgroup of both $Fm\bar{3}m$ and *Cmcm*), whereas the third one is reconstructive (*Cmcm* is not subgroup of $Pm\bar{3}m$).

In addition to the intrinsic interest of its complex high-pressure polymorphism, another important reason for a theoretical study of the AgCl system is related to the fact that, for different substances where the direct rock salt-type to CsCl-type reconstructive transformation is observed (e.g., many alkali halides and alkaline-earth oxides), a transition pathway was proposed which is based just on a $P2_1/m$ intermediate state with KOH-type structure.[7−9] Quantum mechanical calculations showed that a secondary minimum of the enthalpy is attained along the transformation path of the $P2_1/m$ state, predicting an intermediate metastable state with the TlI-type structure between the equilibrium rock salt and CsCl-type end phases.[7,8] This orthorhombic structure was also suggested to be possibly intermediate between the two cubic ones by geometric considerations.[13] Therefore, a close relationship is proven in this case between postulated intermediate states of reconstructive phase transitions in a particular system, and metastable or even stable thermodynamic phases in a different similar system.

On the theoretical side, a computational investigation of AgCl and the other silver halides is present in the literature,[14] where the rock salt to CsCl-type transformation is suggested to occur continuously via an intermediate state which is an idealized version of the cinnabar structure ($P3_121$). This model is clearly at variance with the established experimental results reported above.

Method of Calculation

The quantum mechanical total energy per unit cell of the various polymorphs of AgCl was calculated by means of the computer code CRYSTAL03.[15] This is based on the periodic LCAO (linear combination of atomic orbitals) approach, where the SCF (self consistent field) equations for one-electron eigenvalues and crystalline orbitals are solved by use of the Hartree−Fock or the DFT (density functional theory) Hamiltonian, or even of appropriate mixtures of them. Here, the DFT-GGA (generalized gradient approximation)-PBE functional was employed.[16] Silver atoms were represented by a Hay−Wadt small core pseudopotential[17] accounting for 36 inner electrons and by 22 localized atomiclike functions of type 311(sp)31-(d)G accounting for the outer electron shells. Chlorine atoms are represented by a Hay−Wadt large core pseudopotential and by 12 atomic orbitals of type 311(sp)G. As usual, the radial factors are expressed as linear combinations of Gaussian-type functions of the electron-nucleus distance. The Gaussian parameters were taken from ref 18, but the exponents of the outer sp and d-type functions were reoptimized by minimizing the total energy at the experimental room-pressure rock salt-type structural configuration (Ag(sp), 0.1637; Ag(d), 0.1927; Cl(sp), 0.1422 bohr^{-2}). Tolerances related to cutoff limits for series summation were set to 10^{-7}, 10^{-7}, 10^{-7}, and 10^{-7}. The reciprocal space was sampled according to a regular sublattice defined by 8 points in the Monkhorst grid (from 125 to 170 points in the irreducible Brillouin zones of the different polymorphs considered). Convergence was checked with respect both to tolerances and to the number of Monkhorst points, and it was controlled by a threshold ($\Delta E = 10^{-10}$ hartree per primitive unit cell) in the SCF cycles. To accelerate the SCF convergence, the technique of level shifter was used: that enhances the energy difference between highest occupied and lowest empty states in the first cycles.

Atomic coordinates were optimized by calculation of analytical gradients and a subsequent conjugate gradients algorithm. The unit cell optimizations were performed by the LoptCG routine written by C. Zicovich-Wilson, which is based on computation of numerical derivatives of the total energy with respect to unit cell constants and subsequent processing by conjugate gradients. The routine was modified so as to minimize the enthalpy H at a given pressure, rather than the energy at zero pressure as in the ordinary case. The technique of classifying the mono- and bielectronic integrals according to a reference structure (FIXINDEX option of the code) was employed, to reduce the numerical noise of enthalpy curves calculated for structures with different volumes. A reference volume of 32.63 Å^3 per AgCl formula unit, much smaller than those of all the structures considered, was used in all cases; the actual reference structures were obtained by rescaling their unit cells so as to reduce the volume accordingly.

Results and Discussion

The Phase Equilibria. Figure 1 shows the rock salt-, TlI-, and CsCl-type structures, emphasizing the monoclinic unit cell which can be used as a common reference frame and which also represents the lattice of the KOH-type structure. The latter has not been shown explicitly, but is just a slight monoclinic distortion of the orthorombic TlI structure. The monoclinic reference cell can be obtained from the conventional ones of the three phases of Figure 1 by the following transformation matrices: [$^1/_2$ $^1/_2$ 0 / $-^1/_2$ $-^1/_2$ 0 / 0 0 1], [1 0 0 / 0 0 −1 / $-^1/_2$ $^1/_2$ 0], and [1 0 0 / 0 1−1 / −1 1 1] for rock salt, TlI, and CsCl-type, respectively. It ensues that, if one wants to obtain the monoclinic lattice constants of the higher-symmetry structures (cf. below), the following relationships should be used: $a = b = a(Fm\bar{3}m)/\sqrt{2}$, $c = a(Fm\bar{3}m)$, $\beta = 90°$; $a = a(Cmcm)$, $b = c(Cmcm)$, $c = [a(Cmcm)^2 + b(Cmcm)^2]^{1/2}/2$, $\cos\beta = -a(Cmcm)/[a(Cmcm)^2 + b(Cmcm)^2]^{1/2}$; $a = a(Pm\bar{3}m)$, $b = a(Pm\bar{3}m)\sqrt{2}$, $c = a(Pm\bar{3}m)\sqrt{3}$. This monoclinic cell has been chosen consistent with that used in ref 11 for the KOH-type phase of AgCl, and that employed in the kinetic study[8] of NaCl is related to it by the transformation [1 0 1 / 0 −1 0 / 1 0 0].

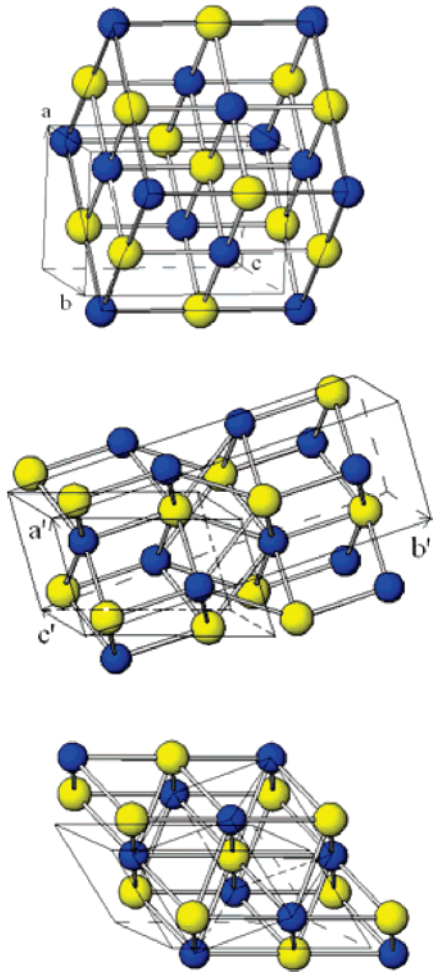

Figure 1. Crystal structures of the rock salt-type (top, $Fm\bar{3}m$), TlI-type (middle, *Cmcm*), and CsCl-type (bottom, $Pm\bar{3}m$) phases of AgCl, showing also the monoclinic unit cell of the KOH-type ($P2_1/m$) phase which can be used as a common reference frame.

To determine the theoretical pressure stability ranges of the four AgCl polymorphs, the enthalpy of each of them was minimized with respect to all structural degees of freedom at several p values in the 0−25 GPa range. In addition to the unit cell constants, there are two free atomic coordinates (y(Ag) and y(Cl)) in the TlI-type structure, and four (x(Ag), z(Ag), x(Cl) and z(Cl)) in the KOH-type case. The four $H(p)$ curves obtained have been referred to that of the rock salt phase, and they are shown in separate diagrams for the lower (Figure 2) and higher (Figure 3) pressure ranges. The enthalpy of rock salt is then plotted as a dotted horizontal zero line. The condition of thermodynamic stability is attained, in a given p range, for the phase whose enthalpy curve is lowest; phase transitions occur at the equilibrium pressures p_t for which two curves cross each other, so that $\Delta H(p_t)=0$.

On first considering Figure 2, we see that the order of stability of the rock salt, KOH and TlI-type phases with increasing pressure is predicted correctly. The analytic behavior of the curves in the neighborhood of the rock salt/KOH and KOH/TlI-type crossing points should throw light onto the thermodynamic character of the corresponding phase transitions, which seem both to be second-order or weakly first-order. In view of the quite small energy differences involved, on the order of fractions of millielectron volts, it is hard to detect a numerically significant slope discontinuity of the enthalpy at the curve merging points. Let us then look at Figures 4−6, where the behavior of the lattice parameters in the monoclinic reference

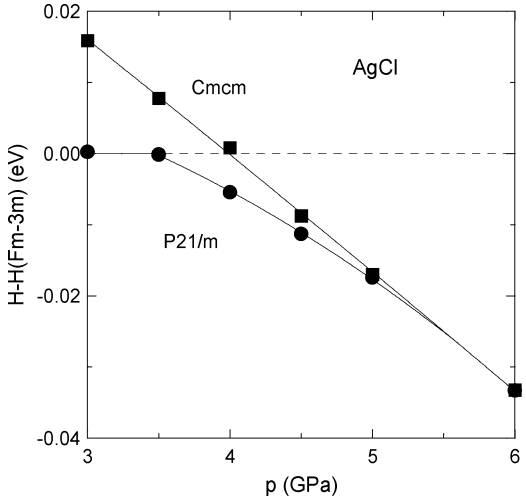

Figure 2. Calculated enthalpies per formula unit of the KOH-type ($P2_1/m$) and TlI-type (*Cmcm*) phases of AgCl, referred to that of the rock salt-type phase, plotted in the lower pressure range.

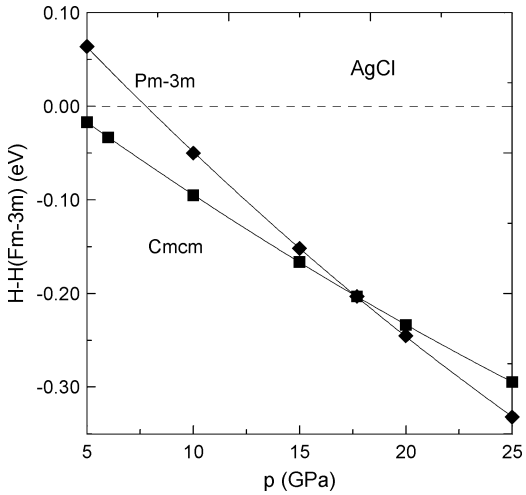

Figure 3. Calculated enthalpies per formula unit of the TlI-type (*Cmcm*) and CsCl-type ($Pm\bar{3}m$) phases of AgCl, referred to that of the rock salt-type phase, plotted in the higher pressure range.

frame, and of the volume per AgCl formula unit, is shown vs pressure for all phases. We see now that both phase transitions are characterized by small but detectable discontinuities of the unit cell constants and volume. Clearer jumps seem to be presented by the monoclinic β angle (Figure 5). However, one should perform very accurate calculations in the neighborhood of the apparent discontinuity to fully clarify the question.

The predicted unit cell constants and volume are compared with the experimental results of ref 11 in Figures 4, 5, and 6. The general aspect of the curves is very similar, but for a downward pressure shift of a few gigapascals characterizing the theoretical with respect to measured data. Hence, the two phase transitions, bracketing the stability field of the KOH-type phase, are calculated to occur at 3.5 and 6 GPa according to our results, against the values of 6.6 and 10.8 GPa given in ref 11. Such discrepancies are not unusual in these calculations: the equilibrium pressure of the rock salt/CsCl-type phases of NaCl was predicted to be 26.3 GPa,[8] versus an experimental value of 29−30 GPa.[19,20] A discussion on possible inaccuracies of structural simulations vs pressures, related to the approximations in the DFT functionals, has been reported elsewhere.[21] In the present case, also the use of pseudopotentials instead of all-electron basis sets for the Ag and Cl atoms should be taken into account. However, a possible overestimation of the

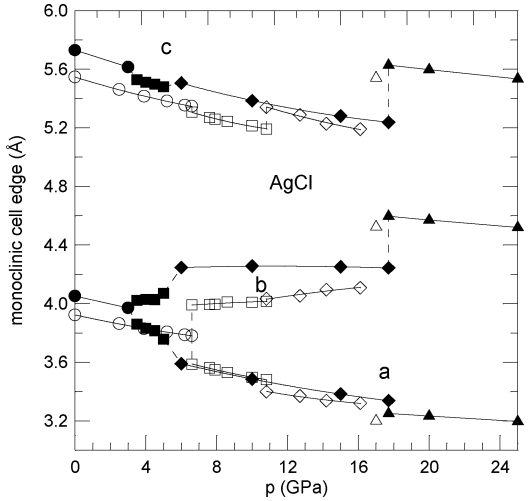

Figure 4. Theoretical (closed symbols) and experimental (open symbols; all data from ref 11, but for those[10] at 17 GPa) unit cell edges of the cubic rock salt- (circles), monoclinic KOH- (squares), orthorhombic TlI- (diamonds), and cubic CsCl- (triangles) type phases of AgCl, all referred to the monoclinic frame of the KOH structure for comparison.

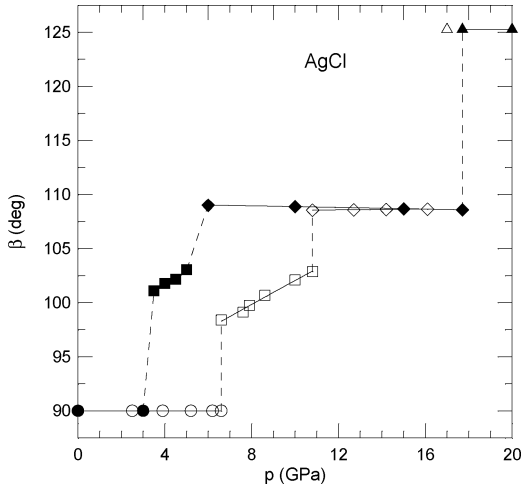

Figure 5. Theoretical (closed symbols) and experimental (open symbols, cf. Figure 4) β angles of the monoclinic reference frame for the cubic rock salt- (circles), monoclinic KOH- (squares), orthorhombic TlI- (diamonds) and cubic CsCl- (triangles) type phases of AgCl.

experimental transition pressures cannot be excluded, in view of the well-known technical problems involved in diamond anvil cell experiments. In this respect, it is noteworthy that the previous experimental paper[10] reported even higher transition pressures (8 and 13 GPa).

Experimental results show discontinuous jumps of the unit cell constants and volume at both phase transitions, with two-phase coexistence at the equilibrium pressure, so as to support a first-order character of the transformations. The effect seems to be quite small for the monoclinic to orthorhombic transition, but more evident for the other transformation (cf. the *a* and *b* behavior). Of course, possible experimental errors due to deviations from hydrostatic conditions, too short equilibration time, or too quick pressure change may affect the observed discontinuities, similarly to the transition pressures as discussed above.

In Figure 3, the TlI- and CsCl-type enthalpy curves in the higher-pressure range are reported, whose crossing point at 17.7 GPa indicates a clean first-order character of the phase transition, consistent with its reconstructive nature. The authors of ref 11

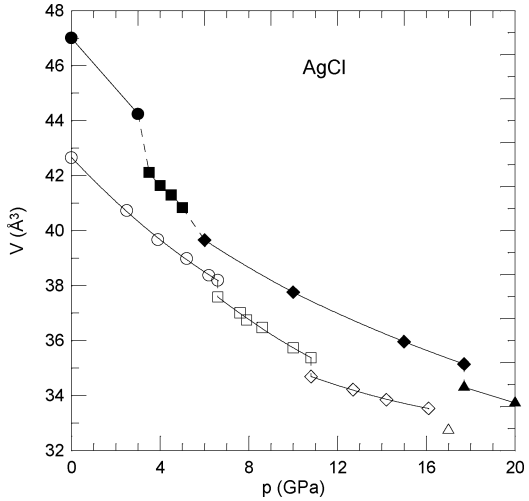

Figure 6. Theoretical (closed symbols) and experimental (open symbols, cf. Figure 4) volume per formula unit of the cubic rock salt-type (circles), monoclinic KOH-type (squares), orthorhombic TlI-type (diamonds), and cubic CsCl-type (triangles) phases of AgCl.

did not observe the *Cmcm*−*Pm*$\bar{3}$*m* transformation, as the pressure of 16 GPa was not exceeded in their experiment. On the other hand, in the previous experiment[10] that transition was located just at 17 GPa, then very close to our predicted value. The jumps of unit cell constants and volume at the transition point are very evident from the theoretical results in Figures 4, 5, and 6.

Kinetic Pathway of the TlI- to CsCl-Type Phase Transition. The mechanism of the reconstructive transformation from the *Cmcm* to the *Pm*$\bar{3}$*m* structure has been investigated at the equilibrium pressure of 17.7 GPa, and at two further *p* values below and above p_t (15.2 and 20.2 GPa). This transition corresponds to the second part of the direct *Fm*$\bar{3}$*m* to *Pm*$\bar{3}$*m* conversion as observed, for instance, in NaCl at 29 GPa, according to a mechanism based on a $P2_1/m$ intermediate state with the KOH-type structure. In the case of NaCl, this mechanism was studied theoretically[8] and found to have a lower activation enthalpy than the mechanism proposed in ref 22 and based on a *Pmmn* intermediate state. Further, about halfway into the $P2_1/m$ pathway, a metastable phase with the TlI-type structure was predicted by theory, in surprising analogy with the sequence of stable phases observed in the AgCl case. It is therefore quite reasonable to assume the KOH-type ($P2_1/m$) structure as the intermediate state of the TlI- to CsCl-type phase transformation of silver chloride.

The monoclinic β angle is taken as the order parameter, ranging from the value obtained for the *Cmcm* structure (108.58° at 17.7 GPa) to that of 125.26° corresponding to the *Pm*$\bar{3}$*m* cubic symmetry. Seven intermediate β values were considered, and for each of them, the $P2_1/m$ structure was optimized by enthalpy minimization with respect to all other structural parameters (three unit-cell edges and four atomic fractional coordinates), keeping the pressure constant. The $\Delta H(\beta, p)$ enthalpy curves obtained are shown in Figure 7, assuming the enthalpy of the *Cmcm* phase at each pressure as reference zero. All three curves display a single maximum, indicating a well-defined bottleneck state whose height gives the activation enthalpy of the transformation. At the equilibrium pressure of 17.7 GPa, the enthalpy barrier is 0.011 eV. This value is substantially smaller than the 0.048 eV obtained for the corresponding transformation in NaCl, though at a higher pressure. Thus, the AgCl system is confirmed to be much softer than sodium chloride. Further, the kinetic enthalpy profile appears to be slightly asymmetrical, with the

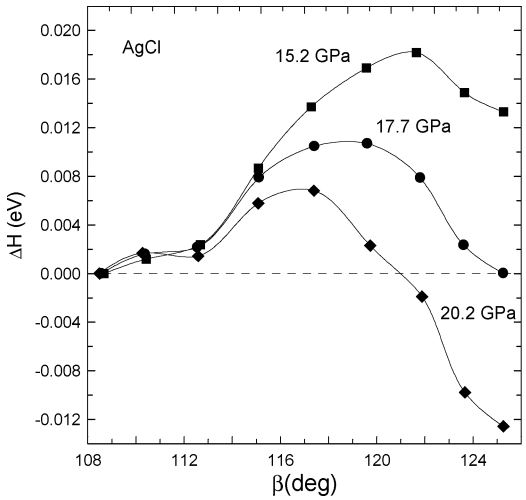

Figure 7. Calculated enthalpy per formula unit, referred to that of the *Cmcm* end phase, of the $P2_1/m$ intermediate state of AgCl along the TlI-type (*Cmcm*) to CsCl-type ($Pm\bar{3}m$) transformation path, plotted vs the monoclinic β angle (order parameter) at three different pressures.

bottleneck state located over halfway at about $\beta = 119°$, and an initial regime on the *Cmcm* side where the system responds very compliantly to the shear strain of the monoclinic cell. At the nonequilibrium *p* values of 15.2 and 20.2 GPa, we observe the irreversible transformation pathway from a metastable to a stable phase (from $Pm\bar{3}m$ to *Cmcm* and from *Cmcm* to $Pm\bar{3}m$, respectively), which illustrates what happens in the case of hysteresis phenomena, so common in the experimental practice. The corresponding activation enthalpies are 0.005 and 0.007 eV, respectively, much lower than the equilibrium value as expected.

An analysis of the changes of interatomic distances and angles along the transformation path, which is not reported here for brevity, shows similar results to those found in the previous study of NaCl for the mechanism of the overall $Fm\bar{3}m$ to $Pm\bar{3}m$ transition. These can be summarized by looking at Figure 1 (top), where three (001) atomic layers of the rock salt structure are displayed: let them be named 1, 2, and 3 from left to right. On passing from rock salt to TlI-type, the relative position of layers 1 and 2 does not change, whereas layers 3 and 4 slide together with respect to layer 2 by [$^1/_4$ $^1/_4$ 0] (cubic reference frame). Therefore, the *Cmcm* structure is obtained from rock salt by relative shifts of alternate pairs of (slightly distorted) fcc layers, by half of the face-centering vector. The second step, from TlI-type to CsCl-type, corresponds to the reconstructive kinetic pathway of AgCl which we are interested in here: it occurs by shifting layer 1 with respect to 2, and layer 4 with respect to 3, whereas the pairs 2−3, 4−5, 6−7, ..., approximately do not change. The relative shifts of pairs of fcc layers correspond to shear deformations of the monoclinic unit cell in two steps: β changes from 90° ($Fm\bar{3}m$) to 108.7° (*Cmcm*) and from 108.7° (*Cmcm*) to 125.3° ($Pm\bar{3}m$). One should notice that the *Cmcm* β value is exactly halfway between those of the two cubic end phases.

Conclusions

The performance of first-principles calculations in simulating the structural, thermodynamic, and kinetic aspects of phase transitions have been illustrated by an application to the complex high-pressure polymorphism of silver chloride. In this case, the monoclinic KOH-type structure, which appears as a nonequilibrium intermediate state of the rock salt/CsCl-type reconstructive transformation of NaCl (according to a previously suggested mechanism), becomes a stable phase in a defined pressure range. The same occurs for the metastable TlI-type structure of the NaCl case. Therefore, the direct rock salt/CsCl-type transition splits into two displacive and one reconstructive phase transformations. The subtle features of these processes have been predicted satisfactorily by the calculations, including the corresponding equilibrium pressures; however, further very accurate work will be needed to clarify in detail the weak first-order character of the two displacive phase transitions. An investigation of the TlI- to CsCl-type reconstructive transformation has confirmed that the atomic pathway is the same as that of the second part of the direct rock salt/CsCl-type conversion of NaCl, though with a much lower activation enthalpy.

Acknowledgment. A financial support from a MIUR-PRIN-2003 (Roma) grant is gratefully acknowledged.

References and Notes

(1) Landau, L. D.; Lifschitz, E. M. *Statistical Physics*; Pergamon: London, 1958.
(2) Toledano, J. C.; Toledano, P. *The Landau Theory of Phase Transitions*; World Scientific: Singapore, 1987.
(3) Buerger, M. In *Phase Transformations in Solids*; Smoluchowski, R., Mayers, J. E., Weyl, W. A., Eds.; Wiley: New York, 1948.
(4) Toledano, P.; Dmitriev, V. *Reconstructive Phase Transitions*; World Scientific: Singapore, 1996.
(5) Limpijumnong S.; Lambrecht, W. R. L. *Phys. Rev. Lett.* **2001**, *86*, 91−94.
(6) Catti, M. *Phys. Rev. Lett.* **2001**, *87*, 035504.
(7) Catti, M. *Phys. Rev. B* **2003**, *68*, 100101(R).
(8) Catti, M. *J. Phys.: Condens. Matter* **2004**, *16*, 3909−3921.
(9) Stokes, H. T.; Hatch, D. M. *Phys. Rev. B* **2002**, *65*, 144114.
(10) Kusaba, K.; Syono, Y.; Kikegawa, T.; Shimomura, O. *J. Phys. Chem. Solids* **1995**, *56*, 751−757.
(11) Hull, S.; Keen, D. A. *Phys. Rev. B* **1999**, *59*, 750−761.
(12) Phillips, J. C. *Rev. Mod. Phys.* **1970**, *42*, 317−356.
(13) Sowa, H. *Acta Crystallogr., Sect. A* **2000**, *56*, 288−299.
(14) Nunes, G. S.; Allen, P. B.; Martins, J. L. *Phys. Rev. B* **1998**, *57*, 5098−5105.
(15) Saunders, V. R.; Dovesi, R.; Roetti, C.; Orlando, R.; Zicovich-Wilson, C. M.; Harrison, N. M.; Doll, K.; Civalleri, B.; Bush, I. J.; D'Arco, Ph.; Llunell, M. *CRYSTAL03: User's manual*; University of Torino, Italy, and CLRC Daresbury Laboratory, U.K., 2003.
(16) Perdew, J. P.; Burke, K.; Ernzerhof, M. *Phys. Rev. Lett.* **1996**, *77*, 3865−3868.
(17) Wadt, W. R.; Hay, P. J. *J. Chem. Phys.* **1985**, ***82***, 284−298.
(18) http://www.crystal.unito.it/Basis_Sets/ptable.html.
(19) Bassett, W. A.; Takahashi, T.; Mao, H. K.; Bell, P. M. *J. Appl. Phys.* **1968**, *39*, 319−325.
(20) Heinz, D. L.; Jeanloz, R. *Phys. Rev. B* **1984**, *30*, 6045−6050.
(21) Catti, M. *Phys. Chem. Miner.* **2001**, *28*, 729−736.
(22) Watanabe, M.; Tokonami, M.; Morimoto, N. *Acta Crystallogr., Sect. A* **1977**, *33*, 294−298.